# Small-signal modeling of wind farm with direct-drive PMSG using the component connection method

Yu, Jie; Li, Jian; Hu, Weihao; Zhang, Guozhou; Wang, Hao; Huang, Qi; Chen, Zhe

*Published in:*
Energy Reports

*DOI (link to publication from Publisher):*
10.1016/j.egyr.2021.01.061



*Publication date:*
2021

*Document Version*
Publisher's PDF, also known as Version of record

Available online at www.sciencedirect.com
ScienceDirect
Energy Reports 7 (2021) 334–342
www.elsevier.com/locate/egyr

2020 The International Conference on Power Engineering (ICPE 2020), December 19–21, 2020, Guangzhou, China

# Small-signal modeling of wind farm with direct-drive PMSG using the component connection method

Jie Yu[a], Jian Li[a], Weihao Hu[a,*], Guozhou Zhang[a], Hao Wang[b], Qi Huang[a], Zhe Chen[b]

[a] *Sichuan Provincial Key Lab of Power System Wide Area Measurement and Control, School of Mechanical and Electrical Engineering, University of Electronic Science and Technology of China, Chengdu, China*
[b] *Department of Energy Technology, Aalborg University, Aalborg, Denmark*

Received 24 January 2021; accepted 24 January 2021

**Abstract**

In order to analysis the small signal stability of the direct-drive permanent magnetic synchronous generator (PMSG) based wind farm, this paper makes a small signal model of the windfarm including a detailed model of PMSG adopting a component connection method (CCM). In the process, the system, consist of wind turbine units with PMSG, collection cable, feeder, transmission cable and grid side, is divided into several subsystems. The interconnection between different subsystems is represented by a linear algebra matrix. Then, through integrating the model of each block and the interconnection matrix, the state space matrix of wind farm can be easier to be built. Based on this model, eigenvalue trajectory is applied to analysis control parameters of the wind turbines to achieve better dynamic performance of the system. A simulation model based on MATLAB/SIMULINK of a two by two wind turbines (WT) wind farm is presented as a test system to validate the effectiveness of CCM.



Peer-review under responsibility of the scientific committee of the International Conference on Power Engineering, ICPE, 2020.

*Keywords:* CCM; State space matrix; Eigenvalue trajectory; MATLAB/SIMULINK

## 1. Introduction

In recent years, wind energy has been widely applied to power generation. Different from fossil fuel, Wind energy is a renewable resource with abundant reserves and broad commercial prospects. Among different type wind turbines, doubly fed induction generator (DFIG) and permanent magnetic synchronous generator (PMSG) have a high degree of market recognition. In particular, PMSG is more adaptable to low wind speed, with less energy consumption and lower follow-up maintenance cost. However, because of the increasing capacity of wind farm and the fluctuating characteristics of wind speed that have a big effect on the stability of the system, more attention should be paid to the small stability of the PMSG based wind farm.

* Corresponding author.
*E-mail address:* whu@uestc.edu.cn (W. Hu).

https://doi.org/10.1016/j.egyr.2021.01.061

Peer-review under responsibility of the scientific committee of the International Conference on Power Engineering, ICPE, 2020.

Many previous researches about small signal stability of wind farm focus on the analysis of a detailed wind turbine unit model building in a small system [1–3], or the influence of wind farm on connected power system, ignoring dynamics of generators [4,5], or just the layout of wind farm while simplifying the wind turbine as a source [6]. However, it has taken less concern for the small signal model of the whole wind farm considering both cable network connection and detailed wind turbine unit at the same time. Jhih-Siang Yang derived the linearized frequency control model of an islanding system include an equivalent synchronous generator and an equivalent DFIG in [1]. In [2], authors presented how DFIG based wind farm affects the small signal stability of system that added distributed load in the western system coordinating council (WSCC) 3-machine 9-bus system. In [3], a model of PMSG-based wind turbine connected to power grid is built and simulated in MATLAB/Simulink. In [5], a wind farm was modeled as a multi-input multi-output (MIMO) dynamic system, and the effect of phase-locked loop (PLL) and the time-delay of digital control systems are considered. A derived stability limit has been used for the stability analysis in [6] to approximately indicate the potential instability risk of wind farm with simplified PMSGs dominated by the dynamics of PLLs.

This paper focuses on adopting a component connection method (CCM) to build a complete model of the wind farm of large dimensions. CCM has the nature of that fixing the problems in formulating complex system matrix [7] and is often used in harmonic stability analysis [8,9]. Comparing traditional modeling method, it greatly reduces the modeling difficulty and can be easily extend to a more complex and larger wind farm system. In this paper, a small signal model of the wind farm with detailed descriptions of PMSG and cable network was successful established by using CCM. The main contributions are: (1) a small-signal model of the wind turbine with direct-drive PMSG in wind farm is build, consist of wind turbine, PMSG, converters, controllers, filter and an ideal transformer. (2) The small signal model of cable network considering type $\pi$ cable was build. (3) CCM is used to simplify the process of wind farm modeling. (4) Eigenvalue trajectory analysis method is applied to optimize controller parameters to increase the system stability.

The rest parts of this paper are designed as follows: Section 2 defines wind farm structure. In Section 3, the system model modeled by CCM is given. Section 4 shows the simulation results. Section 5 concludes this paper.

## 2. System structure

Due to the large dimension of small signal model of the wind farm, it is difficult to be directly used in calculation. However, this process can be simplified by adopting CCM. To better show this method, a four wind turbines (1 MW) based wind farm is firstly designed, with the layout of two by two, which is shown in Fig. 1.

Fig. 1 shows a schematic diagram of PMSG based wind farm system. The wind turbine generators are divided into two groups connected by the inter-array and the distance of wind turbine between each group is set to 0.882 km. Besides, there is a feeder behind each inter-array, equal to 1 km, which is employed to collect the output power of each branch, and transmit the power to the grid. The cable between feeders and the grid adopts transmission cable, which is set as 21 km. Besides, each wind turbine unit contains the wind turbine, PMSG, converters, filter and an ideal transformer.

### 2.1. Model of wind turbine

The dynamics can be expressed as the following equations:

$$\begin{cases} T_{wi} = \frac{C_{Pi}\rho\pi R_i^2 V_{wi}^3}{2\omega_{mi}} \\ C_{Pi} = 0.22(\frac{116}{\gamma_i} - 0.4\beta - 5)e^{-12.5/\gamma_i} \\ \frac{1}{\gamma_i} = \frac{1}{\lambda_i + 0.08\beta^2} - \frac{0.035}{\beta^3+1} \end{cases} \tag{1}$$

where "$i$" represents $i$th wind turbine, $i = 1, 2, 3, 4$, $\rho$ is the air density, $V_{wi}$ is wind speed, $R_i$ is the blade radius, $\omega_{mi}$ is the angular speed of wind turbine, $C_{Pi}$ is the power efficient, which is related with tip velocity ratio $\lambda_i$ ($\lambda_i = \omega_{mi} R_i / V_{wi}$) and pitch angle $\beta$.

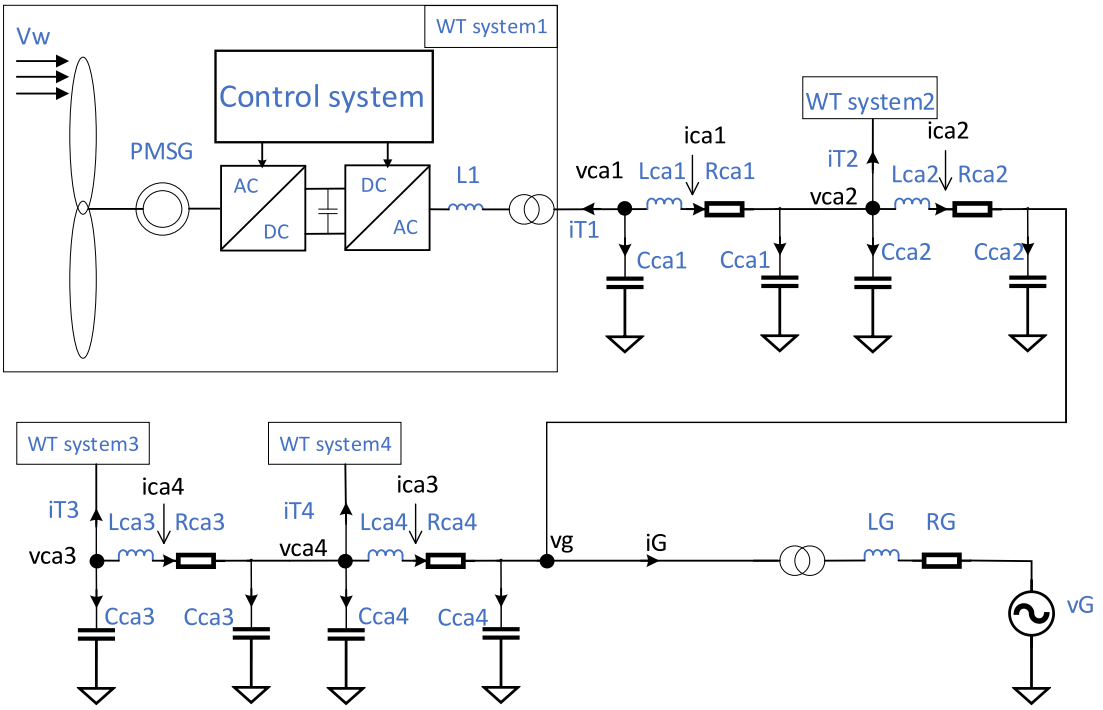


**Fig. 1.** Diagram of wind farm structure.

## 2.2. Model of PMSG

The dynamics model can be expressed as follows:

$$\begin{cases} u_{sdi} = -R_{si} i_{sdi} + \omega_{ei} L_{si} i_{sqi} - L_{si} P i_{sdi} \\ u_{sqi} = -R_{si} i_{sqi} - \omega_{ei} L_{si} i_{sdi} - L_{si} P i_{sqi} + \omega_{ei} \psi_{pmi} \end{cases} \tag{2}$$

$$T_{ei} = \frac{3}{2} n_p \psi_{pm} i_{sqi} \tag{3}$$

where $P$ is the differential operator, $u_{sdi}$ and $u_{sqi}$ is the direct ($d$) and quadrature ($q$) axis stator voltage, respectively, $i_{sdi}$ and $i_{sqi}$ is $d$ and $q$ stator current, respectively, $T_{ei}$ is electrical torque, $\omega_{ei} = n_p \omega_{mi}$ is the generator electrical speed, $n_p$ is the number of poles, $\psi_{pmi}$ is the magnet flux linkage. And the dynamic equation (3) can be transformed into per-unit forms as follows:

$$\begin{cases} \overline{u}_{sdi} = -\overline{R}_{si} \overline{i}_{sdi} + \overline{\omega}_{ei} \overline{L}_{si} \overline{i}_{sqi} - \overline{L}_{si} \overline{P} \overline{i}_{sdi} \\ \overline{u}_{sqi} = -\overline{R}_{si} \overline{i}_{sqi} - \overline{\omega}_{ei} \overline{L}_{si} \overline{i}_{sdi} - \overline{L}_{si} \overline{P} \overline{i}_{sqi} + \overline{\omega}_{ei} \overline{\psi}_{pmi} \end{cases} \tag{4}$$

where $\overline{a}$ represents per-unit value of variable a, and the base values of the relevant variable can be seen in Table 1.

## 2.3. Model of drive train

While the rotor is connected to generator, the mechanical system can be modeled as:

$$J_i P \omega_{mi} = T_{wi} - T_{ei} \tag{5}$$

where $J_i$ is the equivalent inertia time constant. The Eq. (5) can be rewritten to the form as follows:

$$J_i \omega_B \overline{P} \omega_i = T_{wi} - T_{ei} \tag{6}$$

where $\omega_B$ is the base value of angular velocity.

### 2.4. Model of grid side

Similar to the model of PMSG, the equation of grid side in per-unit forms can be derived as follows:

$$\begin{cases} \overline{u}_{kdi} = \overline{u}_{gdi} - \overline{L}_i \overline{P}\, \overline{i}_{gdi} + \overline{\omega}_i \overline{L}_i \overline{i}_{gqi} \\ \overline{u}_{kqi} = \overline{u}_{gqi} - \overline{L}_i \overline{P}\, \overline{i}_{gqi} - \overline{\omega}_i \overline{L}_i \overline{i}_{gdi} \end{cases} \tag{7}$$

where $\omega_i$ is the electrical angular of the ac voltage connected to the grid-side converter.

### 2.5. Model of converters and controllers

Fig. 2(a) illustrates the generator-side converter control, reference value of $i_{sdi}$ ($i^*_{sdi}$) is set as 0 and $i^*_{sqi}$ refer to the current that matches the maximal input of the wind turbine torque. Fig. 2(b) shows the grid-side converter control, the reference direction of grid-side current $i_{gi}$ is from grid to the converter. $d$ axis current is controlled to 0 to obtain 0 reactive power ($Q_{gi}$) and $q$-axis current $i_{gqi}$ is controlled to stabilized capacitor voltage ($U_{dci}$).

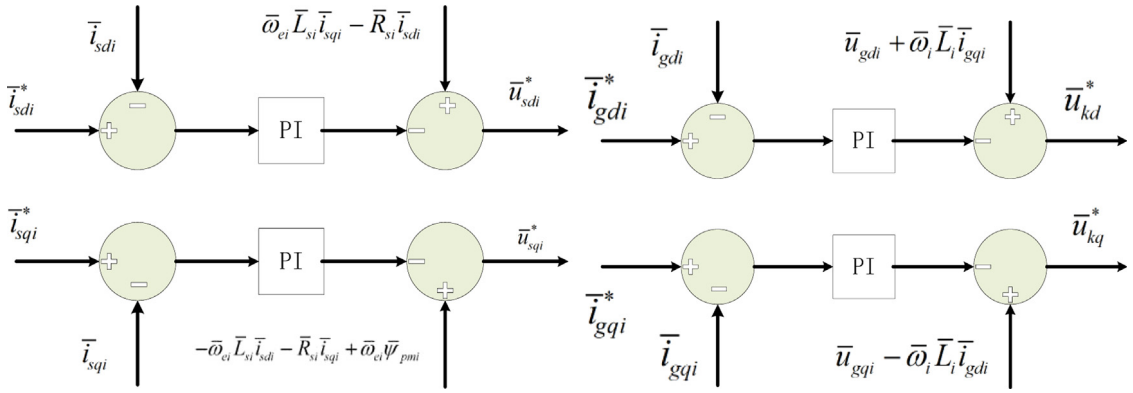


**Fig. 2.** (a) Diagram of the generator-side converter control; (b) Diagram of the grid-side converter control.

The control equations of generator side and grid side are as follows:

$$\begin{cases} \overline{i}^*_{sdi} = 0 \\ \overline{P}\varphi_{1i} = \overline{i}^*_{sdi} - \overline{i}_{sdi} \\ \overline{u}^*_{sdi} = -K_{P1i}\left(\overline{i}^*_{sdi} - \overline{i}_{sdi}\right) - K_{I1i}\varphi_{1i} + \overline{\omega}_{ei}\overline{L}_{si}\overline{i}_{sqi} - \overline{R}_{si}\overline{i}_{sdi} \\ \overline{i}^*_{sqi} = \dfrac{2T^*_{ei}}{3n_p\psi_{pmi}i_B} \\ T^*_{ei} = \dfrac{C_{Pmax}\rho\pi R_i^3 V_{wi}^2}{2\lambda_{opt}} \\ \overline{P}\varphi_{2i} = \overline{i}^*_{sqi} - \overline{i}_{sqi} \\ \overline{u}^*_{sqi} = -K_{P2i}\left(\overline{i}^*_{sqi} - \overline{i}_{sqi}\right) - K_{I1i}\varphi_{2i} - \overline{\omega}_{ei}\overline{L}_{si}\overline{i}_{sdi} + \overline{\omega}_{ei}\overline{\psi}_{pmi} - \overline{R}_{si}\overline{i}_{sqi} \end{cases} \tag{8}$$

$$\begin{cases} \overline{i}^*_{gdi} = 0 \\ \overline{P}\varphi_{3i} = \overline{i}^*_{gdi} - \overline{i}_{gdi} \\ \overline{u}^*_{kdi} = -K_{P3i}\left(\overline{i}^*_{gdi} - \overline{i}_{gdi}\right) - K_{I3i}\varphi_{3i} + \overline{\omega}_i\overline{L}_i\overline{i}_{gqi} + \overline{u}_{gdi} \\ \overline{P}\varphi_{4i} = \overline{U}^*_{dci} - \overline{U}_{dci} \\ \overline{i}^*_{gqi} = K_{P4i}(\overline{U}^*_{dci} - \overline{U}_{dci}) + K_{I4i}\varphi_{4i} \\ \overline{P}\varphi_{5i} = \overline{i}^*_{gqi} - \overline{i}_{gqi} \\ \overline{u}^*_{kqi} = -K_{P5i}\left(\overline{i}^*_{gqi} - \overline{i}_{gqi}\right) - K_{I5i}\varphi_{5i} - \overline{\omega}_i\overline{L}_i\overline{i}_{gdi} + \overline{u}_{gqi} \end{cases} \tag{9}$$

where $\varphi_{1i}, \varphi_{2i}, \varphi_{3i}, \varphi_{4i}, \varphi_{5i}$ are intermediate variables, $K_{p1i}, K_{p2i}, K_{p3i}, K_{p4i}, K_{p5i}, K_{I1i}, K_{I2i}, K_{I3i}, K_{I4i}, K_{I5i}$ are the constants in the PI block. Ignoring the dynamic process of converter, $u^*_{sdi} = u_{sdi}, u^*_{sqi} = u_{sqi}, u^*_{kdi} = u_{kdi}, u^*_{kqi} =$

$u_{kqi}$. From Eqs. (4), (7), (8) and (9), Eq. (10) can be obtained.

$$\begin{cases} \overline{L}_{si}\overline{P}\,\bar{\imath}_{sdi} = K_{P1i}(\bar{\imath}^{*}_{sdi} - \bar{\imath}_{sdi}) + K_{I1i}\varphi_{1i} \\ \overline{L}_{si}\overline{P}\,\bar{\imath}_{sqi} = K_{P2i}(\bar{\imath}^{*}_{sqi} - \bar{\imath}_{sqi}) + K_{I2i}\varphi_{2i} \\ \overline{L}_{i}\overline{P}\,\bar{\imath}_{gdi} = K_{P3i}(\bar{\imath}^{*}_{gdi} - \bar{\imath}_{gdi}) + K_{I3i}\varphi_{3i} \\ \overline{L}_{i}\overline{P}\,\bar{\imath}_{gqi} = K_{P5i}(\bar{\imath}^{*}_{gqi} - \bar{\imath}_{gqi}) + K_{5i}\varphi_{5i} \end{cases} \tag{10}$$

### 2.6. Model of direct current voltage

The model of DC-link in per-unit form can be derived as follows:

$$\overline{C}_{i}\overline{U}_{dci}\overline{PU}_{dci} = \overline{u}_{sdi}\bar{\imath}_{sdi} + \overline{u}_{sqi}\bar{\imath}_{sqi} + \overline{u}_{gdi}\bar{\imath}_{gdi} + \overline{u}_{gqi}\bar{\imath}_{gqi} \tag{11}$$

### 2.7. Model of complete wind turbine unit

Linearizing (6)–(11) around a steady state, the complete dynamic model of wind turbine system can be written in the following form:

$$\begin{cases} \overline{P}\Delta x_{wi} = A_{wi}\Delta x_{wi} + B_{wi}u_{wi} \\ \Delta y_{wi} = C_{wi}\Delta x_{wi} + D_{wi}u_{wi} \end{cases} \tag{12}$$

where $x_{wi} = \left[\overline{\omega}_{mi}, \overline{i_{sdi}}, \overline{i_{sqi}}, \overline{\varphi_{1i}}, \overline{\varphi_{2i}}, \overline{\varphi_{3i}}, \overline{\varphi_{4i}}, \overline{\varphi_{15i}}, \overline{i_{gdi}}, \overline{i_{gqi}}, \overline{U_{dci}}\right]^{T}$, $u_{wi} = \left[V_{wi}, \overline{u_{gdi}}, \overline{u_{gqi}}\right]^{T}$, $y_{wi} = \left[\overline{i_{sdi}}, \overline{i_{sqi}}, \overline{i_{gdi}}, \overline{i_{gqi}}\right]^{T}$

### 2.8. Model of cable network

The cable network consists of collection cable, feeder, transmission cable and grid side. The transformers are viewed as ideal transformers. Fig. 1 shows the electrical circuit of the cable network, which takes the terminal grid voltage $v_G$ as the reference voltage. Based on the electrical circuit above, the dynamic model of the cable network can be written as:

$$\begin{cases} \overline{C}_{ca1}\overline{P}\,\overline{v}_{ca1} = -\bar{\imath}_{ca1} - \bar{\imath}_{T1} \\ \overline{C}_{ca12}\overline{P}\,\overline{v}_{ca2} = \bar{\imath}_{ca1} - \bar{\imath}_{ca2} - \bar{\imath}_{T2} \\ \overline{C}_{ca3}\overline{P}\,\overline{v}_{ca3} = -\bar{\imath}_{ca3} - \bar{\imath}_{T3} \\ \overline{C}_{ca34}\overline{P}\,\overline{v}_{ca4} = \bar{\imath}_{ca3} - \bar{\imath}_{ca4} - \bar{\imath}_{T4} \\ \overline{C}_{ca24}\overline{P}\,\overline{v}_{g} = \bar{\imath}_{ca2} + \bar{\imath}_{ca4} - \bar{\imath}_{G} \end{cases} \quad \begin{cases} \overline{L}_{ca1}\overline{P}\,\bar{\imath}_{ca1} = \overline{v}_{ca1} - \overline{v}_{ca2} - \overline{R}_{ca1}\bar{\imath}_{ca1} \\ \overline{L}_{ca2}\overline{P}\,\bar{\imath}_{ca2} = \overline{v}_{ca2} - \overline{v}_{g} - \overline{R}_{ca2}\bar{\imath}_{ca2} \\ \overline{L}_{ca3}\overline{P}\,\bar{\imath}_{ca3} = \overline{v}_{ca3} - \overline{v}_{ca4} - \overline{R}_{ca3}\bar{\imath}_{ca3} \\ \overline{L}_{ca4}\overline{P}\,\bar{\imath}_{ca4} = \overline{v}_{ca4} - \overline{v}_{g} - \overline{R}_{ca4}\bar{\imath}_{ca4} \\ \overline{L}_{G}\overline{P}\,\bar{\imath}_{G} = \overline{v}_{g} - \overline{v}_{G} - \overline{R}_{G}\bar{\imath}_{G} \end{cases} \tag{13}$$

where $\overline{C_{ca12}} = \overline{C_{ca1}} + \overline{C_{ca2}}$, $\overline{C_{ca34}} = \overline{C_{ca3}} + \overline{C_{ca4}}$, $\overline{C_{ca24}} = \overline{C_{ca2}} + \overline{C_{ca4}}$. By linearizing (13), the small signal equations can be written as follows:

$$\begin{cases} \overline{P}\Delta x_{net} = A_{net}\Delta x_{net} + B_{net}u_{net} \\ \Delta y_{net} = C_{net}\Delta x_{net} + D_{net}u_{net} \end{cases} \tag{14}$$

where $x_{net} = \left[\overline{v_{ca1DQ}}, \overline{v_{ca2DQ}}, \overline{v_{ca3DQ}}, \overline{v_{ca4DQ}}, \overline{v_{g1DQ}}, \overline{i_{ca1DQ}}, \overline{i_{ca2DQ}}, \overline{i_{ca3DQ}}, \overline{i_{ca4DQ}}, \overline{i_{G1DQ}}\right]^{T}$, $u_{net} = \left[\overline{i_{T1DQ}}, \overline{i_{T2DQ}}, \overline{i_{T3DQ}}, \overline{i_{T4DQ}}, \overline{\omega}\right]^{T}$, $y_{net} = \left[\overline{v_{ca1DQ}}, \overline{v_{ca2DQ}}, \overline{v_{ca3DQ}}, \overline{v_{ca4DQ}}, \overline{i_{GDQ}}\right]^{T}$.

## 3. System modeling based on CCM

The models of each subsystem have been built. Considering relationship of subsystems' interconnection, the system model can be built by adopting CCM.

### 3.1. CCM

The nonlinear differential equations often used to represent the dynamics of $i$th component, which is shown as follows:

$$\begin{cases} x_i = f(x_i, u_i) \\ y_i = g(x_i, u_i) \end{cases} \tag{15}$$

where $x_i, y_i, u_i$ are the vector of states, output and input of $i$th component, respectively. According to Taylor series expansion theory, the linearized models can be derived as:

$$\begin{cases} \dot{x}_i = A_i x_i + B_i u_i \\ y_i = C_i x_i + D_i u_i \end{cases} \tag{16}$$

Because the state space models of each units are in parallel, a combined state space matrix is formed by integrating the units' models together as given below:

$$\begin{cases} \dot{x}_T = A_T + A_T u_T \\ y_T = C_T x_T + D_T u_T \end{cases} \tag{17}$$

where $A_T, B_T, C_T, D_T$ are system matrixes, $x_T, y_T, u_T$ are the state, output and input variables, separately. $A_T = diag(A_1 \cdots A_n), B_T = diag(B_1 \cdots B_n), C_T = diag(C_1 \cdots C_n), D_T = diag(D_1 \cdots D_n), x_T = [x_1 \cdots x_n]^T, u_T = [u_1 \cdots u_n]^T, y_T = [y_1 \cdots y_n]^T$.

Moreover, according to the linear interconnection relationship between each part's input and output can be attained. Fig. 3 shows the partitioned system and the relationship between the components. Eqs. (18) can be formed to describe it.

$$\begin{cases} u_T = M_1 y_T + M_2 a \\ b = M_3 y_T + M_4 a \end{cases} \tag{18}$$

where $a$ and $b$ represent the system inputs and outputs. $M_1, M_2, M_3, M_4$ are modules interconnection matrixes. Then, based on the basis of Eqs. (15) and (16), the system state space model can be obtained.

$$\begin{cases} \dot{x}_T = H x_T + I a \\ b = J x_T + K a \end{cases} \tag{19}$$

where $H = A_T + B_T (I - M_1)^{-1} M_1 C_T, I = B_T (I - M_1 D_T)^{-1} M_2, J = M_3 (I - D_T M_1)^{-1} C_T, K = M_3 D_T (I - M_1 D_T)^{-1} M_2 + M_4$. Then, the system small stability can be analyzed via the state matrix $H$.

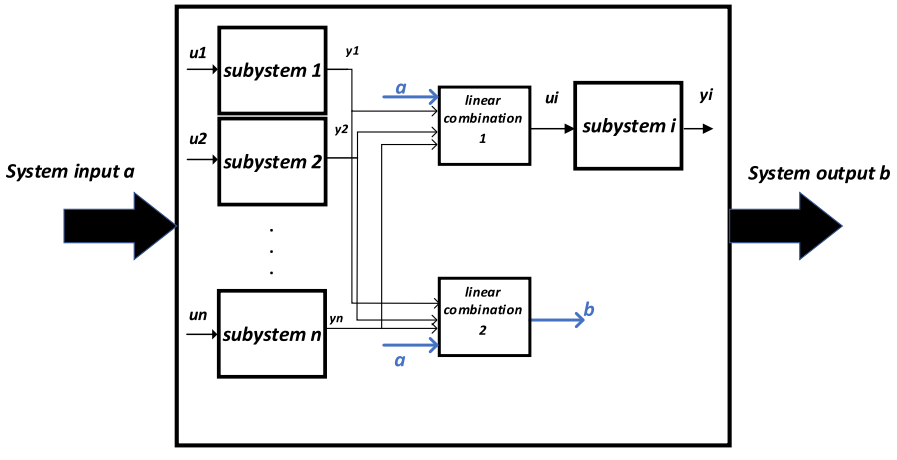


**Fig. 3.** Diagram of subsystem interconnection.

### 3.2. System modeling

The wind farm system includes 2 types of subsystems, and (13) and (15) have described its small signal model, so what needs to be added is modules' interconnection matrixes. Cable network system regards $v_G$ as the reference voltage, while small signal model of wind turbine unit $i$ takes $u_{gi}$ as the reference voltage. The angle of two $d-q$ axis reference frames can be derived as follows:

$$\theta_i = \arctan\left(\overline{v}_{GQ0}/\overline{v}_{GD0}\right) - \arctan(\overline{u}_{gqi0}/\overline{u}_{gdi0}) \tag{20}$$

The conversion relations of the relevant voltages or currents in two $d-q$ axis is indicated as follows:

$$\begin{cases} \overline{u}_{gdqi} = \begin{bmatrix} cos\theta_i & sin\theta_i \\ -sin\theta_i & cos\theta_i \end{bmatrix} \overline{v}_{caiDQ} \\ \overline{\imath}_{TiDQ} = \begin{bmatrix} cos\theta_i & -sin\theta_i \\ sin\theta_i & cos\theta_i \end{bmatrix} \overline{\imath}_{gdqi} \end{cases} \tag{21}$$

Set $A_T = diag\left(A_{w1}, A_{w2}, A_{w3}, A_{w4}, A_{net}\right)$, $B_T = diag\left(B_{w1}, B_{w2}, B_{w3}, B_{w4}, B_{net}\right)$, $C_T = diag\left(C_{w1}, C_{w2}, C_{w3}, C_{w4}, C_{net}\right)$, $D_T = diag\left(D_{w1}, D_{w2}, D_{w3}, D_{w4}, D_{net}\right)$, $x_T = \left[x_{w1}^T, x_{w2}^T, x_{w3}^T, x_{w4}^T, x_{net}^T\right]^T$, $u_T = \left[u_{w1}^T, u_{w2}^T, u_{w3}^T, u_{w4}^T, u_{net}^T\right]^T$, $y_T = \left[y_{w1}^T, y_{w2}^T, y^T, y_{w4}^T, y_{net}^T\right]^T$, $a = [\Delta V_{w1}, \Delta V_{w2}, \Delta V_{w3}, \Delta V_{w4}, \Delta\overline{\omega}]^T$, $b = \left[\Delta\overline{\imath}_{GD}, \Delta\overline{\imath}_{GQ}\right]^T$. Then, interconnection matrixes $M_1, M_2, M_3, M_4$ can be obtained. According to (20), $H, I, J, K$ can be derived and models of subsystems are integrated into an overall system model.

$$\begin{cases} \overline{P}\Delta x = H\Delta x_T + Ia \\ b = J\Delta x_T + Ka \end{cases} \tag{22}$$

Thus, it can be seen that it is much easier to get the system model based on subsystems' model once you figure out the interconnection matrix.

## 4. Simulation

A time-domain simulation is constructed in SIMULINK to verify the small signal model and the effectiveness of the optimization algorithm, and the parameters of the test system is listed in Table 1. Part of wind turbine generator data refer to [3] and some cable network data refer to [9].

**Table 1**. The test system parameters.

| Variable of base | Value | Variable of wind turbines | Value | Variable of cable network | Value |
|---|---|---|---|---|---|
| $S_B$ (MVA) | 1.5 | $n_p$ | 48 | $L_{ca1,3}$ (mH) | 0.36 |
| $U_{WTB}$ (V) | $690\sqrt{2}/\sqrt{3}$ | $\rho$ (kg/m$^3$) | 1.237 | $L_{ca2,4}$ (mH) | 0.35 |
| $U_{caB}$ (KV) | $35\sqrt{2}/\sqrt{3}$ | $\lambda_{opt}$ | 6.33 | $L_G$ (mH) | 7.6 |
| $U_{GB}$ (KV) | $110\sqrt{2}/\sqrt{3}$ | $\psi_{pmi}$ | 2 | $R_{ca1,3}$ (Ω) | 0.185 |
| $U_{dcB}$ (V) | 1200 | $C_{pmax}$ | 0.44 | $R_{ca1,4}$ (Ω) | 0.078 |
| $\omega_B$ | $100\pi$ | $R_{si}$ (Ω) | 0.007 | $R_G$ (Ω) | 10 |
| | | $L_{si}$ (mH) | 0.395 | $C_{ca1,3}$ (μF) | 0.185 |
| | | $L_i$ (mH) | 0.607 | $C_{ca1,4}$ (μF) | 0.29 |
| | | $C_i$ (F) | 0.01 | | |

Fig. 4 shows the simulation results of state space model and the time-domain model of the wind farm, and $t = 0$ s, a small signal that $V_{w1} = 11$ m/s changes to 12 m/s is given. The relevant variables, $\bar{\imath}_{GQ}$ is observed. The responses are similar and because of the filter that led to longer overshoot time and smaller minimum peak, there is a little difference in $\bar{\imath}_{GQ}$, which proves the accuracy of the model. It means that CCM can be used to model the wind farm.

To analyze the small signal stability, the eigenvalue trajectory can be used to observe the influence of $K_{p21}$. Because of high dimensional properties of matrix about 64 dimensions, it is better to only show the dominant poles. In Fig. 5, the eigenvalue is presented when the machine-side controller parameter $K_{p21}$ increase from 1 to 100.

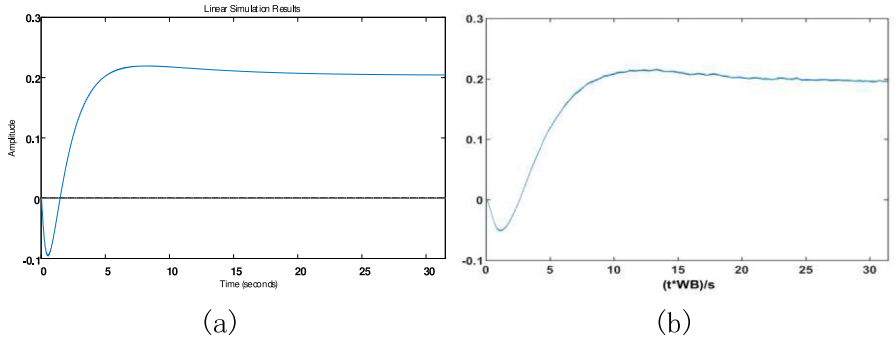


**Fig. 4.** (a) Diagram of $i_{GDQ}$ in the state space model; (b) Diagram of $i_{GDQ}$ in the time-domain model.

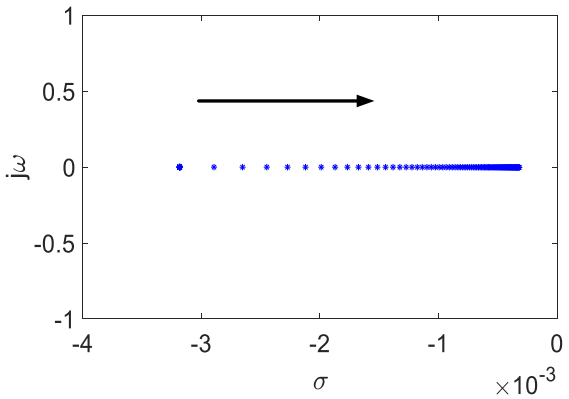


**Fig. 5.** Diagram of root locus with $K_{p21}$ increasing.

Analysis result represents that as the increase of $K_{p21}$, the dominant poles moves to the imaginary axis. Based on this, it is illustrated that the performance of the system with control parameters $K_{p21}$, $K_{p22}$, $K_{p23}$, $K_{p24}$ are equal to 1 or 5 when $V_{w1}$, $V_{w2}$, $V_{w3}$, $V_{w3} = 11$ m/s changes to 12 m/s. From Fig. 6, it can be observed that the minimum peak gets bigger, which proves the validity of the eigenvalue trajectory analysis method.

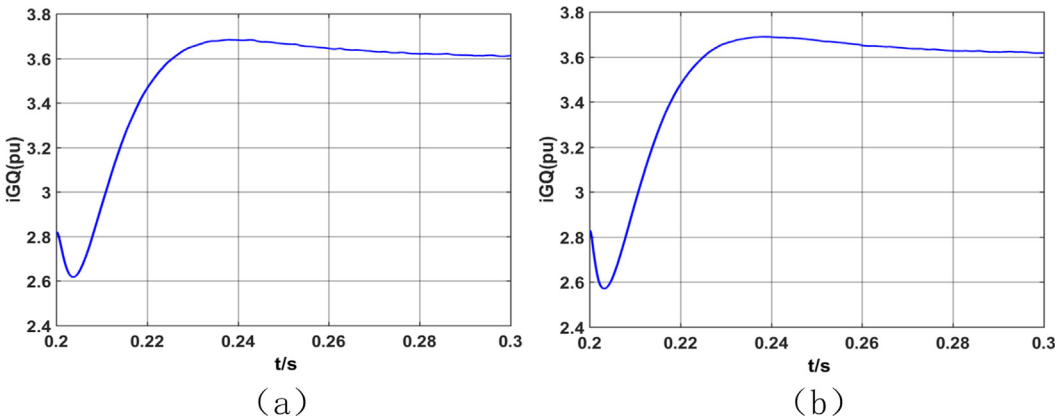


**Fig. 6.** (a) Diagram of $i_{GDQ}$ when $K_{p2i} = 1, i = 1, 2, 3, 4$; (b) Diagram of $i_{GDQ}$ when$K_{p2i} = 5, i = 1, 2, 3, 4$.

## 5. Conclusion

In the paper, a CCM is proposed to reduce the modeling difficulty of the designed wind farm system, which considering both detailed PMSG model and cable network. In the study, both the model of PMSG and cable network is established and can be also studied independently. Based on the models of the two kinds of subsystems, a system model of a PMSG based wind farm is built and the small signal stability has been analyzed. Moreover, eigenvalue trajectory analysis method is applied to optimize the small signal stability of the study system. The simulation is conducted in the MATLAB/SIMULATION to verified the model and analysis method. But because of the oscillation of the time domain simulation model, there are still some differences between the observed time-domain simulation signal processed by the filter and the signal in the state space. And a wind farm with a large number of wind turbine generators is not designed in the modeling study, which will be consider in the future research.

## Declaration of competing interest

The authors declare that they have no known competing financial interests or personal relationships that could have appeared to influence the work reported in this paper.

## Acknowledgment

The authors gratefully acknowledge the support by the Natural Science Foundation of China (NFSC, Grant No. 51977025).

## References

[1] Yang J, Chen Y, Hsu Y. Small-signal stability analysis and particle swarm optimisation self-tuning frequency control for an islanding system with DFIG wind farm. IET Gener Transm Dist 2019;13(4):563–74. http://dx.doi.org/10.1049/iet-gtd.2018.6101.

[2] Weyman-Jones Thomas, Boucinha Júlia Mendonça, Inácio Catarina Feteira. Measuring electric energy efficiency in portuguese households: a tool for energy policy. Manag Environ Qual Int J 2015;26(3):407–22.

[3] Huang H, Mao C, Lu J, Wang D. Small-signal modelling and analysis of wind turbine with direct drive permanent magnet synchronous generator connected to power grid. IET Renew Power Gener 2012;6(1):48–58. http://dx.doi.org/10.1049/iet-rpg.2010.0217.

[4] Wang T, Gao M, Mi D, Huang S, Wang Z. Dynamic equivalent method of PMSG-based wind farm for power system stability analysis. IET Gener Transm Dist 2020;14(17):3488–97. http://dx.doi.org/10.1049/iet-gtd.2020.0006.

[5] Ebrahimzadeh E, et al. Small signal modeling of wind farms. In: 2017 IEEE energy conversion congress and exposition (ECCE), Cincinnati, OH. 2017, p. 3710–6. http://dx.doi.org/10.1109/ECCE.2017.8096656.

[6] Du W, Dong W, Wang HF. Small-signal stability limit of a grid-connected PMSG wind farm dominated by the dynamics of PLLs. IEEE Trans Power Syst 2020;35(3):2093–107. http://dx.doi.org/10.1109/TPWRS.2019.2946647.

[7] Wang Y, Wang X, Chen Z, Blaabjerg F. Small-signal stability analysis of inverter-fed power systems using component connection method. IEEE Trans Smart Grid 2018;9(5):5301–10. http://dx.doi.org/10.1109/TSG.2017.2686841.

[8] Wang Y, Wang X, Chen Z, Blaabjerg F. Small-signal stability analysis of inverter-fed power systems using component connection method. IEEE Trans Smart Grid 2018;9(5):5301–10. http://dx.doi.org/10.1109/TSG.2017.2686841.

[9] Hou P, Ebrahimzadeh E, Wang X, Blaabjerg F, Fang J, Wang Y. Harmonic stability analysis of offshore wind farm with component connection method. In: IECON 2017-43rd annual conference of the IEEE industrial electronics society, Beijing. 2017, p. 4926–32. http://dx.doi.org/10.1109/IECON.2017.8216850.